LG-DBGL: Lateralization-Guided Dissociative Brain Graph Learning for Alzheimer's Disease Identification

Jiazhen Ye[1], Manman Yuan[1](✉), Junlin Li[2], Weiming Jia[1], Jiacheng Wang[1], and Jiapei Li[1]

[1] School of Computer Science, Inner Mongolia University, Hohhot, 010021, China
jiazhenye@mail.imu.edu.cn,yuanman@imu.edu.cn
[2] Department of Imaging Medicine, Inner Mongolia Autonomous Region People's Hospital, Hohhot, 010017, China

Abstract. Thanks to advances in neuroimaging, graph neural networks (GNNs) have emerged as a powerful tool for learning brain graph representations to identify Alzheimer's Disease (AD). However, existing methods often overlook the brain's hemispherical lateralization, enforcing homogeneous information propagation between hemispheres, which limits their learning capabilities. In this study, we propose a novel dissociative brain graph learning framework (LG-DBGL) guided by brain lateralization to enhance AD identification. Specifically, the Lateralized Decoupling (LD) module partitions brain networks into left/right hemispheric and cross-hemispheric sub-networks. The Dissociative Graph Encoder (DGE) module then independently learns representations for each sub-network, preserving lateralized functional features and avoiding feature confusion. Finally, the Multi-Source Fusion Mechanism (MSFM) dynamically quantifies the contribution of each sub-network to AD-related pathological features, enabling lateralization-guided multi-source feature fusion. Comprehensive experiments conducted on a real-world dataset demonstrate the effectiveness of our LG-DBGL. Our code is publicly available at https://github.com/ilove-gh/LG-DBGL.

Keywords: Alzheimer's disease · Brain graph learning · Brain lateralization, Graph neural network.

1 Introduction

Alzheimer's Disease (AD) is a complex neurodegenerative disorder characterized by cognitive decline and language deficits, significantly impairing the quality of life in elderly populations [9,6]. Recent advances in neuroimaging have enabled the representation of the brain as a brain graph (or brain network) based on neuroimaging data [22,14]. To further our understanding, identification, treatment, and exploration of AD, graph neural networks (GNNs) [10,3,26] have been developed to learn representations of these brain networks, capturing structural and functional connections within the brain [21,30,28]. This approach provides a rich basis for analyzing AD and has emerged as a promising tool for its identification.

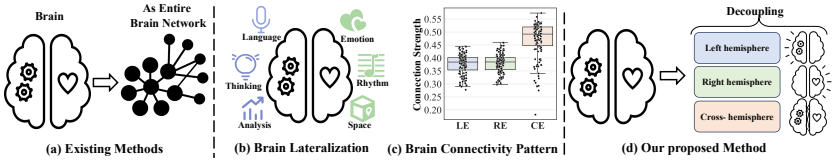

Fig. 1. Brain lateralization in the brain network. (a) Existing methods treat the brain as an entire brain network. (b) Hemispheric lateralization of the brain. (c) The connection strengths of the left intra-hemisphere, right intra-hemisphere, and cross-hemisphere edges (i.e., LE, RE, and CE) of 120 subjects were generated by DTI on the ADNI dataset. (d) Our method decouples the brain network into three parts via lateralization.

From the view of cognitive decline in patients, the key challenge in brain graph learning for AD identification is to capture the critical pathological features related to diseases from brain networks. For instance, some studies analyze brain networks in specific states to identify AD-related abnormal features [23,28]. In contrast, others track changes across different time points or tasks to uncover dynamic alterations [15,12]. Moreover, multimodal brain graph learning integrates various imaging modalities (e.g., Diffusion Tensor Imaging (DTI), functional Magnetic Resonance Imaging (fMRI)) to reveal disease-related features comprehensively [13,27]. However, these methods feed the entire brain network into the model (Fig. 1(a)), ignoring the issue of hemispherical lateralization.

In clinical settings, hemispherical lateralization is a crucial and significant characteristic that emerges through developmental processes and manifests as distinct functional specializations between the left and right hemispheres [25,11], as shown in Fig. 1(b). For example, the left hemisphere primarily handles language processing and logical inference [4,18], while the right hemisphere is more involved in spatial cognition and emotional processing [19,24]. In patients with AD, regions associated with language in the left hemisphere often exhibit significant changes due to cognitive decline [8,7]. Moreover, this functional differentiation results in intrinsic differences in information transfer patterns between intra-hemispheric and inter-hemispheric connections [17,20], a phenomenon empirically validated in real biological datasets, detailed in Fig. 1(c). Therefore, the methods that consider the brain network as a whole but neglect the factor of hemispherical lateralization will restrict the model's ability to learn critical pathological features of AD. Specifically, **1) Loss of Functional Specificity**: *Treating both hemispheres with the same information propagation patterns obscures the unique functional roles of the left and right hemispheres.* **2) Blurred Coupling Relationships**: *Equating intra-hemispheric and inter-hemispheric connections blurs their distinct roles in AD progression.* These issues reduce the sensitivity of existing models to brain network degradation, thereby limiting their learning representation capabilities and overall efficacy in identifying AD.

As such, to address these issues, we propose the Lateralization-Guided Dissociative Brain Graph Learning framework (LG-DBGL), whose innovations are

reflected in three aspects: First, The Lateralized Decoupling (LD) module leverages the characteristic of hemispherical lateralization to partition brain networks into left/right hemispheric and cross-hemispheric sub-networks, explicitly modelling lateralized functional features. Second, we design a Dissociative Graph Encoder (DGE) biased towards brain networks that preserve lateralized functional features through independent representation learning for all sub-networks, avoiding feature confusion. Third, we propose a Multi-Source Fusion Mechanism (MSFM) that dynamically quantifies the contribution of each sub-network to AD-related pathological features, enabling multi-source feature fusion. Extensive experiments on the ADNI dataset demonstrate that LG-DBGL significantly outperforms existing benchmark methods in AD identification tasks.

The main contributions of this study can be summarized as follows:

- We propose the dissociative brain network learning paradigm based on the theory of hemispherical lateralization, breaking through the biological rationality limitations of traditional brain graph modelling.
- We develop the DGE and MSFM modules, effectively addressing feature confusion caused by hemispherical lateralization and achieving dissociative brain graph learning.
- A series of experiments on the ADNI dataset validate the superiority of LG-DBGL in AD classification tasks.

2 Methodology

2.1 Problem Formulation

In this study, we construct the brain network using resting-state fMRI and DTI data as the initial node feature matrix and graph structure. Specifically, each brain network is represented as $G = (A, X)$, where $X = \{v_1, ...v_n\} \in R^{n \times d}$ is the node feature matrix extracted from fMRI, with each node v_i characterized by a d-dimension Blood Oxygen Level Dependent (BOLD) time series, and $A \in R^{n \times n}$ is the adjacency matrix. The element $A_{ij} \in [0, 1]$ represents the Fractional Anisotropy (FA) between brain regions i and j, measured by DTI. Here, $A_{ij} = 0$ indicates unrestricted diffusion of water molecules, while $A_{ij} = 1$ signifies highly directional diffusion. Each brain network G is associated with a label $y = \{0, 1\}$, where $y = 0$ denotes a healthy subject and $y = 1$ denotes a subject with the disease. The overall goal is to develop a model that accurately classifies brain networks into their respective groups based on these labels.

2.2 Model Architecture

LG-DBGL overcomes the limitations of existing brain graph learning methods by explicitly modelling hemispherical lateralization, mainly including: (a) Lateralized Decoupling; (b) Dissociative Graph Encoder; (c) Multi-Source Fusion Mechanism. The overall architecture of the LG-DBGL model is shown in Fig. 2.

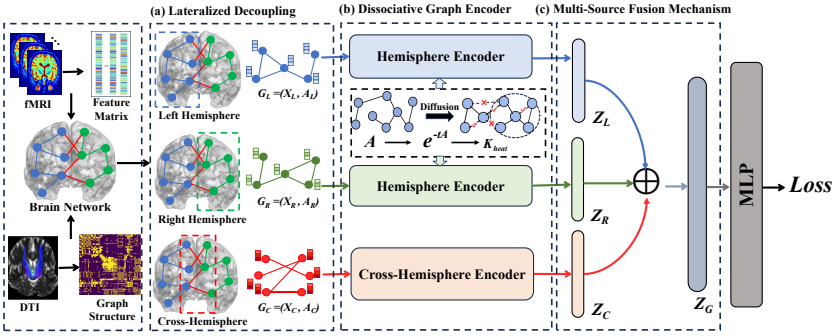

Fig. 2. Overall architecture of LG-DBGL. (a) Lateralized Decoupling; (b) Dissociative Graph Encoder; (c) Multi-Source Fusion Mechanism.

2.3 Lateralized Decoupling (LD)

As mentioned in the Introduction Section, the brain exhibits significant hemispherical lateralization, especially in pathological conditions such as AD. To explicitly model this lateralization and the degraded cross-hemispheric interactions during AD progression, we partition the brain network G into three sub-networks: the left hemisphere G_L, the right hemisphere G_R, and the cross-hemispheric G_C. Let $V = V_L \cup V_R$ with $V_L \cap V_R = \emptyset$, where V_L and V_R denote the set of left/right hemisphere nodes, respectively. Such as the left hemisphere G_L (Similarly definitions for G_R, A_R, and X_R), we define the sub-network node feature matrix as $X_L = \{X_i \mid i \in V_L\}$ and the adjacency matrix A_L as:

$$(A_L)_{i,j} = \begin{cases} A_{i,j}, & \text{if } i,j \in V_L, \\ 0, & \text{otherwise.} \end{cases} \tag{1}$$

To obtain cross-hemispheric G_C, we extract its adjacency matrix via:

$$(A_C)_{i,j} = \begin{cases} A_{i,j}, & \text{if } i \in V_L \text{ , } j \in V_R \text{ or } i \in V_R \text{ , } j \in V_L, \\ 0, & \text{otherwise,} \end{cases} \tag{2}$$

and defined corresponding node feature matrix as $X_C = \{X_k \mid \exists l : (A_C)_{k,l} \neq 0\}$ including all nodes participating in cross-hemispheric edges.

This partition decouples lateralized functional specialization of brains (G_L, G_R) while isolating degenerative cross-hemispheric interactions (G_C) in AD.

2.4 Dissociative Graph Encoder (DGE)

In this section, the DGE preserves lateralized functional features through independent representation learning for G_L, G_R, and G_C. This approach ensures hemisphere-specific feature learning while mitigating cross-sub-network interference. The DGE mainly utilizes two encoding types–hemispherical and cross-hemispherical encoders–to achieve this purpose.

Hemispheric Encoder. Since hemispheric networks in patients with AD may exhibit local connectivity degradation due to the disease, we use heat diffusion to enhance critical pathways of these networks. For the G_L (Similarly with G_R), we calculate the normalized graph Laplacian $\hat{A}_L = I_n - D_L^{-1/2} A_L D_L^{-1/2}$ with the degree matrix $(D_L)_{i,i} = \sum_j (A_L)_{i,j}$. Inspired by graph diffusion network[5], we define the heat kernel as $K_{heat} = e^{-t\hat{A}_L}$ (t is the diffusion time, and weak connections (weight < 0.0001) pruned to reduce noise), to model the diffusion process on the network. To obtain the hemispheric embedding Z_L, we apply a two-layer convolution to aggregate the results via SUM pooling:

$$Z_L = \mathrm{SUM}\big(\sigma\left(K_{heat} \cdot \sigma\left(K_{heat} X_L W_1\right) \cdot W_2\right)\big), \tag{3}$$

where W_1 and W_2 are learnable weights, σ is a RELU activation function. The parameter t balances the trade-off between local and global network structures. Larger t values promote global diffusion and capture broader network structures, while smaller t values preserve local connectivity patterns within the network.

Cross-Hemispheric Encoder. The cross-hemispherical networks G_C exhibit a bipartite-like topology with connections primarily between nodes across hemispheres. Accordingly, we employ a Graph Isomorphism Network (GIN) [26] for its strong capacity in learning discriminative graph representations. At the l-th layer, the hidden feature vector $h_i^{(l)}$ for each node i is updated using the following aggregation function to integrate information from neighbouring nodes:

$$h_i^{(l)} = \mathrm{MLP}\left(\left(1 + \epsilon^{(l)}\right) \cdot h_i^{(l-1)} + \sum_{j \in \mathcal{N}(i)} \left(h_j^{(l-1)}\right)\right), \tag{4}$$

where ϵ is a trainable parameter, $\mathcal{N}(i)$ is the set of neighbouring nodes of i, and $h_i^{(0)} = (X_C)_i$ is the initial feature vector of node i, MLP is a multi-layer perceptron to iteratively conduct for all nodes at l-th layer, followed by pooling together to generate a graph-level representation:

$$Z_C = \sum_{i=1}^{n} h_i. \tag{5}$$

2.5 Multi-Source Fusion Mechanism (MSFM)

Once we obtain the embeddings for all sub-networks, we use MSFM to dynamically quantify each sub-network's contribution to AD, enabling lateralization-guided multi-source feature fusion. Specifically, let $\mathcal{P} = \{Z_L, Z_R, Z_C\}$ be the set of sub-network embeddings, and for each $p \in \mathcal{P}$, the attention coefficient e_p assigned to the sub-network embedding is computed by:

$$e_p = q_p^T \cdot \tanh(W_p \cdot (Z_p)^T + b_p), \tag{6}$$

where q_p is a parameterized vector, W_p is a learnable weight matrix, and b_p is a bias value. These attention coefficients are normalized via softmax to sum to

one, enabling a probabilistic interpretation of each sub-network's contribution.

$$\beta_p = \frac{\exp(e_p)}{\sum_{p' \in \mathcal{P}} \exp(e_{p'})}. \tag{7}$$

Finally, we obtain the final brain network embedding Z_G by taking the weighted sum of all the embeddings using the normalized attention weights:

$$Z_G = \sum_{p \in \mathcal{P}} \beta_p \cdot Z_p. \tag{8}$$

2.6 Objective Loss

Through the modules introduced above, we obtain highly abstracted brain network representations for each subject. After that, the final embedding of Z_G into an MLP to derive the prediction:

$$\hat{y} = \mathrm{MLP}(Z_G). \tag{9}$$

For each sample $t \in \mathcal{T}$, we feed the predicted label $\hat{y}$ and the true label y into the cross-entropy function to compute the prediction loss.

$$\mathcal{L}_s = -\frac{1}{\mathcal{T}} \sum_{\mathcal{T}} \Big(y \cdot \log(\hat{y}) + (1-y) \cdot \log(1-\hat{y}) \Big). \tag{10}$$

3 Experiments

3.1 Experimental Setup

Datasets. We evaluated our LG-DBGL using the publicly accessible Alzheimer's Disease Neuroimaging Initiative (ADNI) dataset [16], which includes 120 subjects: 28 healthy controls (NC), 51 with mild cognitive impairment (MCI), and 41 with AD. MCI is widely recognized as a precursor to AD, making it a critical component in AD-related identification tasks. All subjects received two imaging scans: DTI for brain structure and fMRI for brain functional activity. Further details on preprocessing and subject demographics are available in the GitHub repository referenced in the abstract.

Baselines. We compared our proposed LG-DBGL with several representative methods, including GNN-based methods such as GCN [10], GCNH [1], CAGNN [2], as well as brain graph learning methods for AD identification like Cross-GNN [27], HeBrainGNN [21], BGAN [29], OT-MCSTGCN [30], and MHSA [28]. This selection provides a comprehensive benchmark for evaluating our method.

Implementation Details. Given the relatively small size of the ADNI dataset, we employed 5-fold cross-validation for all experiments to ensure fair comparisons. All methods' performance was evaluated using the mean values of classification Accuracy (ACC), F1-score (F1), and Area Under the Curve (AUC). For our proposed LG-DBGL, the hyperparameters were set as follows: 0.5 dropout

Table 1. The performance of LG-DBGL is compared to competing methods.

Group	Model	NC vs. MCI			NC vs. AD		
		ACC(%)	F1(%)	AUC(%)	ACC(%)	F1(%)	AUC(%)
GCN-Based	GCN	70.92 ± 6.21	67.99 ± 8.82	68.0 ± 12.8	66.59 ± 9.91	62.02 ± 13.78	63.69 ± 12.19
	CAGNN	77.33 ± 6.12	74.56 ± 10.39	73.33 ± 12.69	75.38 ± 14.66	69.33 ± 19.77	69.67 ± 16.94
	GCNH	81.0 ± 6.86	79.13 ± 9.78	77.18 ± 10.84	79.89 ± 9.33	78.57 ± 10.27	77.33 ± 7.74
Brain Network	HeBrainGNN	74.92 ± 10.31	83.64 ± 6.68	65.67 ± 12.89	81.58 ± 5.30	87.18 ± 2.12	73.76 ± 8.94
	OT-MCSTGCN	79.67 ± 5.06	82.49 ± 11.38	66.06 ± 14.01	78.13 ± 5.8	82.43 ± 6.06	68.64 ± 24.01
	BGAN	79.58 ± 9.72	78.0 ± 10.27	73.82 ± 7.53	81.10 ± 3.81	80.89 ± 3.58	77.43 ± 6.23
	MHSA	82.33 ± 7.18	80.08 ± 10.13	77.52 ± 10.90	80.84 ± 5.80	79.60 ± 6.20	75.90 ± 9.42
	Cross-GNN	79.75 ± 4.64	86.37 ± 2.89	71.67 ± 8.94	83.95 ± 8.56	$\mathbf{88.23 \pm 6.26}$	80.08 ± 11.13
Ours	**LG-DBGL**	$\mathbf{88.5 \pm 7.56}$	$\mathbf{87.16 \pm 8.8}$	$\mathbf{83.0 \pm 11.85}$	$\mathbf{85.49 \pm 4.54}$	84.52 ± 5.5	$\mathbf{82.08 \pm 7.14}$

Table 2. Evaluation of the significance of different components of LG-DBGL.

Method	NC vs. MCI			NC vs. AD		
	ACC(%)	F1(%)	AUC(%)	ACC(%)	F1(%)	AUC(%)
w/o MSFM	86.08 ± 8.27	84.07 ± 10.25	79.67 ± 12.93	83.96 ± 5.72	83.56 ± 5.90	82.0 ± 7.01
w/o DGE	83.50 ± 3.30	81.85 ± 4.49	77.67 ± 7.86	76.59 ± 10.25	74.86 ± 11.07	73.42 ± 12.31
w/o LD	75.16 ± 13.76	69.21 ± 19.46	69.58 ± 18.89	70.88 ± 7.06	64.42 ± 12.03	64.08 ± 10.36
LG-DBGL	$\mathbf{88.5 \pm 7.56}$	$\mathbf{87.16 \pm 8.8}$	$\mathbf{83.0 \pm 11.85}$	$\mathbf{85.49 \pm 4.54}$	$\mathbf{84.52 \pm 5.5}$	$\mathbf{82.08 \pm 7.14}$

rate, 0.025 learning rate, weight decay of 1e-4, 500 epochs with patience 30, and 16 hidden units. The diffusion time t was tuned from 1 to 10 in increments of 1. Baseline models were implemented manually in our experimental environment according to the authors' specified parameters. In addition, all experiments were conducted on servers equipped with NVIDIA GeForce RTX 4090 GPUs.

3.2 Results

Classification Results. We evaluated LG-DBGL on two target domain tasks, as detailed in Table 1. Across these tasks, LG-DBGL consistently outperformed competing methods on nearly all metrics. Specifically, for MCI identification, LG-DBGL achieved accuracy improvements of $6.17\% - 17.58\%$, and for AD identification, it demonstrated gains of $1.54\% - 18.9\%$. These results highlight LG-DBGL's robust recognition capabilities across different cognitive stages. The enhanced performance is primarily attributed to LG-DBGL's innovative design, which effectively integrates brain hemispherical lateralization and detailed modelling of complex brain networks, enhancing its efficacy in identifying AD.

Ablation Study. We conducted ablation studies on LG-DBGL's three key components—MSMF, LD, and DGE—to evaluate their contributions to AD-related brain network modelling, as detailed in Table 2. w/o MSMF will equalize the contributions of all sub-networks; w/o DGE will share a simple GCN [10] encoder across sub-networks; and w/o LD will input the entire brain network into the encoder in Eq. 3 without lateralization-based decoupling. Results indicate significant performance drops when any component is removed, with the

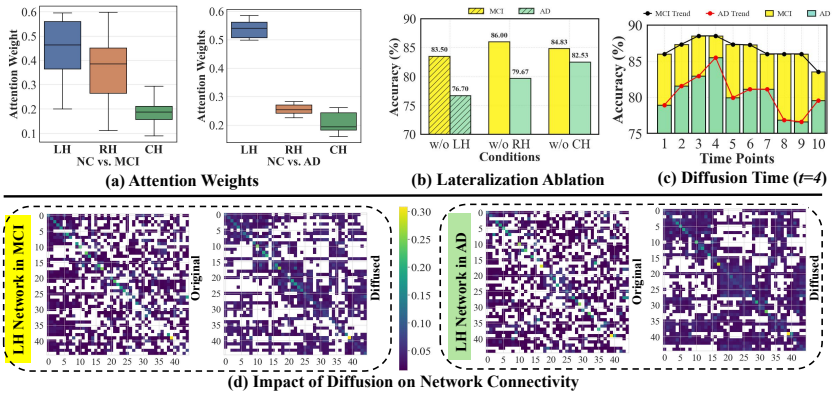

Fig. 3. Visualization of results based on the ADNI dataset. (a) Distribution of attention weights captured by the MSFM module for left/right and cross-hemisphere networks (i.e., LH, RH, and CH). (b) Impact of Ablating left/right and cross-hemisphere networks on model performance. (c) Sensitivity analysis of diffusion time t. (d) Impact of heat diffusion on network connectivity.

most severe declines observed for LD. These findings highlight the importance of leveraging lateralized brain network characteristics for effective pathological feature capture and validating lateralisation's critical role in LG-DBGL's design.

3.3 Discussion Analysis

Lateralization. To investigate the impact of lateralization in AD and MCI identification, we visualized average attention weights for left, right, and cross-hemispheric sub-networks captured by the MSFM module (Fig. 3(a)) and found the left hemisphere's dominant role in MCI and AD identification. Additional ablation studies (Fig. 3(b)) reveal that excluding any sub-network results in a notable decline in model accuracy, with the left hemisphere exhibiting the most significant effect. These results underscore the critical role of left-hemisphere lateralization, consistent with its links to language and cognitive functions.

Heat Diffusion. We analyzed the sensitivity of the heat diffusion time t as mentioned in Section 2.4. Fig. 3(c) shows that the model achieves optimal performance when t is set to 3 or 4. Specifically, smaller t values (e.g., $t = 1$) capture local connectivity but neglect global structure, leading to a slight drop in classification performance. Conversely, larger t values (e.g., $t = 10$) capture global information but may obscure critical local features, negatively impacting the recognition of MCI and AD. To visualize the impact of diffusion time on connectivity, we generated heatmaps of the left hemispherical network (Fig. 3(d)) at $t = 4$, with weights below 0.01 removed to enhance visual clarity. The original network appears disordered, whereas the diffused network shows enhanced local connectivity. This enhancement allows the model to learn richer feature representations.

4 Conclusion

In this paper, we introduce LG-DBGL, a novel brain graph learning framework for AD identification, guided by hemispherical decoupling. LG-DBGL partitions brain networks into lateralized sub-networks and learns their representations independently, thereby capturing unique pathological features and eliminating cross-hemispheric interference. Experiments on the ADNI dataset demonstrate superior performance compared to representative baselines, significantly improving classification accuracy. By decoupling hemispherical lateralization, LG-DBGL not only provides a more nuanced understanding of brain network pathology but also pioneers a new direction in neurodegenerative disease research, opening new avenues for early diagnosis and intervention.

Acknowledgments. This work was supported in part by the National Natural Science Foundation of China under Grant 62466042, in part by the Inner Mongolia University Postgraduate Research and Innovation Project Under Grant 11200-5223737, and in part by the Science and Technology Program of the Joint Fund of Scientific Research for the Public Hospitals of Inner Mongolia Academy of Medical Sciences under Grant 2023GLLH0004.

Disclosure of Interests. The authors have no competing interests to declare that are relevant to the content of this article.

References

1. Cavallo, A., Grohnfeldt, C., Russo, M., Lovisotto, G., Vassio, L.: GCNH: A simple method for representation learning on heterophilous graphs. In: IJCNN. pp. 1–8 (2023)
2. Chen, J., Chen, S., Gao, J., Huang, Z., Zhang, J., Pu, J.: Exploiting neighbor effect: Conv-agnostic gnn framework for graphs with heterophily. IEEE Trans. Neural Netw. Learn. Syst. (2023)
3. Cheng, L., Zhu, P., Gao, C., Wang, Z., Li, X.: A heuristic framework for sources detection in social networks via graph convolutional networks. IEEE Transactions on Systems, Man, and Cybernetics: Systems **54**(11), 7002–7014 (2024)
4. Damasio, A., Bellugi, U., Damasio, H., Poizner, H., Gilder, J.V.: Sign language aphasia during left-hemisphere amytal injection. Nature **322**(6077), 363–365 (1986)
5. Gasteiger, J., Weißenberger, S., Günnemann, S.: Diffusion improves graph learning. In: NeurIPS. vol. 32 (2019)
6. Hansson, O., Jack Jr, C.R.: A clinical perspective on the revised criteria for diagnosis and staging of alzheimer's disease. Nat. Aging. **4**(8), 1029–1031 (2024)
7. Harasty, J., Halliday, G., Xuereb, J., Croot, K., Bennett, H., Hodges, J.: Cortical degeneration associated with phonologic and semantic language impairments in ad. Neurology **56**(7), 944–950 (2001)
8. Hojjati, S.H., Babajani-Feremi, A., Initiative, A.D.N.: Seeing beyond the symptoms: biomarkers and brain regions linked to cognitive decline in alzheimer's disease. Front. Aging Neurosci. **16**, 1356656 (2024)

9. Jack Jr, C.R., Andrews, J.S., Beach, T.G., Buracchio, T., Dunn, B., Graf, A., Hansson, O., Ho, C., Jagust, W., McDade, E., et al.: Revised criteria for diagnosis and staging of alzheimer's disease: Alzheimer's association workgroup. Alzheimers. Dement. **20**(8), 5143–5169 (2024)
10. Kipf, T.N., Welling, M.: Semi-supervised classification with graph convolutional networks. In: ICLR (2017)
11. Liang, H., Gu, Y., Yi, X., Kong, L., Wang, J., Lv, F.: Lateralization study of the basal ganglia, thalamus and supplying arteries in healthy individuals based on structure and connectivity analysis using 7.0 t mri. NeuroImage **306**, 121007 (2025)
12. Liu, J., Cui, W., Chen, Y., Ma, Y., Dong, Q., Cai, R., Li, Y., Hu, B.: Deep fusion of multi-template using spatio-temporal weighted multi-hypergraph convolutional networks for brain disease analysis. IEEE Trans. Med. Imaging. **43**(2), 860–873 (2024)
13. Long, Z., Li, J., Liao, H., Deng, L., Du, Y., Fan, J., Li, X., Miao, J., Qiu, S., Long, C., et al.: A multi-modal and multi-atlas integrated framework for identification of mild cognitive impairment. Brain. Sci. **12**(6), 751 (2022)
14. Luo, X., Wu, J., Yang, J., Xue, S., Beheshti, A., Sheng, Q.Z., McAlpine, D., Sowman, P.F., Giral, A., Yu, P.S.: Graph neural networks for brain graph learning: A survey. In: IJCAI. pp. 8170–8178 (2024)
15. Ma, Y., Cui, W., Liu, J., Guo, Y., Chen, H., Li, Y.: A multi-graph cross-attention-based region-aware feature fusion network using multi-template for brain disorder diagnosis. IEEE Trans. Med. Imaging. **43**(3), 1045–1059 (2024)
16. Mueller, S.G., Weiner, M.W., Thal, L.J., Petersen, R.C., Jack, C.R., Jagust, W., Trojanowski, J.Q., Toga, A.W., Beckett, L.: Ways toward an early diagnosis in alzheimer's disease: The alzheimer's disease neuroimaging initiative (adni). Alzheimer's and Dementia **1**(1), 55–66 (2005)
17. Ocklenburg, S., Guo, Z.V.: Cross-hemispheric communication: Insights on lateralized brain functions. Neuron **112**(8), 1222–1234 (2024)
18. Thiebaut de Schotten, M., Dell'Acqua, F., Forkel, S., Simmons, A., Vergani, F., Murphy, D.G., Catani, M.: A lateralized brain network for visuo-spatial attention. Nat. Neurosci. pp. 1–1 (2011)
19. Sha, Z., Schijven, D., Carrión-Castillo, A., Joliot, M., Mazoyer, B., Fisher, S.E., Crivello, F., Francks, C.: The genetic architecture of structural left–right asymmetry of the human brain. Nat. Hum. Behav. **5**, 1226–1239 (2020)
20. Shi, G., Li, X., Zhu, Y., Shang, R., Sun, Y., Guo, H., Sui, J.: The divided brain: Functional brain asymmetry underlying self-construal. NeuroImage **240**, 118382 (2021)
21. Shi, G., Zhu, Y., Liu, W., Li, X.: A heterogeneous graph based framework for multimodal neuroimaging fusion learning. CoRR **abs/2110.08465** (2021)
22. Sporns, O.: Graph theory methods: applications in brain networks. Dialogues. Clin. Neuro. **20**(2), 111–121 (2018)
23. Wen, G., Cao, P., Bao, H., Yang, W., Zheng, T., Zaiane, O.: Mvs-gcn: A prior brain structure learning-guided multi-view graph convolution network for autism spectrum disorder diagnosis. Comput. Bio. Med. **142**, 105239 (2022)
24. Witelson, S.F.: Sex and the single hemisphere: Specialization of the right hemisphere for spatial processing. Science **193**(4251), 425–427 (1976)
25. Wu, X., Kong, X., Vatansever, D., Liu, Z., Zhang, K., Sahakian, B.J., Robbins, T.W., Feng, J., Thompson, P.M., Zhang, J.: Dynamic changes in brain lateralization correlate with human cognitive performance. PLOS. BIOL. **20**, e3001560 (2022)

26. Xu, K., Hu, W., Leskovec, J., Jegelka, S.: How powerful are graph neural networks? In: ICLR (2019)
27. Yang, Y., Ye, C., Guo, X., Wu, T., Xiang, Y., Ma, T.: Mapping multi-modal brain connectome for brain disorder diagnosis via cross-modal mutual learning. IEEE Trans. Med. Imag. **43**(1), 108–121 (2024)
28. Yuan, M., Jia, W., Luo, X., Ye, J., Zhu, P., Li, J.: Mhsa: A multi-scale hypergraph network for mild cognitive impairment detection via synchronous and attentive fusion. In: BIBM. pp. 2808–2815 (2024)
29. Zhou, Z., Wang, Q., An, X., Chen, S., Sun, Y., Wang, G., Yan, G.: A novel graph neural network method for alzheimer's disease classification. Computers in Biology and Medicine **180**, 108869 (2024)
30. Zhu, Q., Li, S., Meng, X., Xu, Q., Zhang, Z., Shao, W., Zhang, D.: Spatio-temporal graph hubness propagation model for dynamic brain network classification. IEEE Trans. Med. Imaging. **43**(6), 2381–2394 (2024)